



## Article

# Use of Remotely Piloted Aircraft System Multispectral Data to Evaluate the Effects of Prescribed Burnings on Three Macrohabitats of Pantanal, Brazil

Harold E. Pineda Valles <sup>1,\*</sup>, Gustavo Manzon Nunes <sup>1</sup>, Christian Niel Berlinck <sup>2</sup>, Luiz Gustavo Gonçalves <sup>3</sup> and Gabriel Henrique Pires de Mello Ribeiro <sup>4</sup>

- <sup>1</sup> Faculty of Forestry Engineering, Federal University of Mato Grosso, LabSensoR—Remote Sensing and Geotechnologies Laboratory, Postgraduate Program in Forest and Environmental Sciences, Cuiabá Campus, Av. Fernando Corrêa da Costa, 2367, Boa Esperança, Cuiabá 78060-900, MT, Brazil; gustavo.nunes@ufmt.br
- <sup>2</sup> National Research Center for Carnivores Conservation, Chico Mendes Institute for the Conservation of Biodiversity, Estrada Municipal Hisaichi Takebayashi 8600, Atibaia 12952-011, SP, Brazil; christian.berlinck@icmbio.gov.br
- <sup>3</sup> Chapada dos Guimarães National Park, Chico Mendes Institute for the Conservation of Biodiversity, Rodovia Emanuel Pinheiro (MT-251)—km 50, Chapada dos Guimarães 78195-000, MT, Brazil; luiz.gustavo@icmbio.gov.br
- <sup>4</sup> Faculty of Forestry Engineering, Federal University of Mato Grosso, Cuiabá Campus, Av. Fernando Corrêa da Costa, 2367, Boa Esperança, Cuiabá 78060-900, MT, Brazil; gabriel.ribeiro@ufmt.br
- \* Correspondence: hepv\_123@hotmail.com

**Abstract:** The controlled use of fires to reduce combustible materials in prescribed burning helps to prevent the occurrence of forest fires. In recent decades, these fires have mainly been caused by anthropogenic activities. The study area is located in the Pantanal biome. In 2020, the greatest drought in 60 years happened in the Pantanal. The fire affected almost one third of the biome. The objective of this study is to evaluate the effect of prescribed burnings carried out in 2021 on three macrohabitats (M1: natural grassland flooded with a proliferation of *Combretum* spp., M2: natural grassland of seasonal swamps, and M3: natural grassland flooded with a proliferation of *Vochysia divergens*) inside the SESC Pantanal Private Natural Heritage Reserve. Multispectral and thermal data analyses were conducted with remotely piloted aircraft systems in 1 ha plots in three periods of the dry season with early, mid, and late burning. The land use and land cover classification indicate that the predominant vegetation type in these areas is seasonally flooded grassland, with percentages above 73%, except in zone three, which has a more diverse composition and structure, with the presence of arboreal specimens of *V. divergens* Pohl. The pattern of the thermal range showed differentiation pre- and post-burning. The burned area index indicated that fire was more efficient in the first two macrohabitats because they are natural grasslands, reducing the grass species in the burnings. Early and mid prescribed burnings are a good option to reduce the continuous accumulation of dry forest biomass fuel material and help to promote landscape heterogeneity. The use of multispectral sensor data with high spatial/spectral resolution can show the effects of fires, using highly detailed scales for technical decision making.

**Keywords:** burn area index; fire ecology; fire management; remote sensing; thermal band



**Citation:** Pineda Valles, H.E.; Nunes, G.M.; Berlinck, C.N.; Gonçalves, L.G.; Ribeiro, G.H.P.d.M. Use of Remotely Piloted Aircraft System Multispectral Data to Evaluate the Effects of Prescribed Burnings on Three Macrohabitats of Pantanal, Brazil. *Remote Sens.* **2023**, *15*, 2934. <https://doi.org/10.3390/rs15112934>

Academic Editors:  
Fernando Pérez-Cabello and Quazi K. Hassan

Received: 27 March 2023  
Revised: 11 May 2023  
Accepted: 2 June 2023  
Published: 4 June 2023



**Copyright:** © 2023 by the authors. Licensee MDPI, Basel, Switzerland. This article is an open access article distributed under the terms and conditions of the Creative Commons Attribution (CC BY) license (<https://creativecommons.org/licenses/by/4.0/>).

## 1. Introduction

Fire is one of the main factors shaping vegetation [1]. It affects the structure and functions of ecosystems [2] and acts as an evolutionary pressure, not only on pine lineages [3]. It can have a natural origin [4] or it can be caused or instigated by anthropogenic actions [5,6]. In certain ecosystems, fire may be one of the greatest drivers of diversity due to the fire regime, which produces biotic and environmental heterogeneity [7]. Some plant species show a beneficial response based on the natural fire regime [8,9]. Examples

of this are provided in [10]. The response of natural grassland vegetation is positive after the passage of fire, with the regrowth of vegetation and benefits to alpha and gamma diversity and to biodiversity succession processes in areas subjected to prescribed burnings (PB) [11]. Pyrobiodiversity describes the diversity of species and ecosystems related to fire, their adaptation to fire, and the ecological processes that occur during and after a fire [12]. Fire is important for the dynamics of many ecosystems, and pyrobiodiversity is essential for maintaining the health and balance of these ecosystems [13]. Vegetation types can be classified according to their fire recovery response as fire-independent, fire-sensitive, fire-dependent (pyro-resistant), and fire-influenced [14]. The Pantanal biome is classified as fire-dependent, where each phytophysionomy responds differently to the presence of fire [15]. To date, there has been no single fire management strategy for the entire Pantanal biome [16] due to its complexity, floodings, biomass, and land use [17].

The Brazilian Pantanal covers an area of 150,355 km<sup>2</sup> [18]. It is a seasonally flooded sedimentary basin surrounded by plateaus, mountains, and high hills. It is considered the largest seasonal wetland in the world [19]. It is located at the center of the South American continent [20]. The landscape of the Pantanal is defined by the interactions of fires and flood pulses within its ecosystem. Changes in these natural cycles could drastically alter biodiversity [21]. Rainfall plays an important role in flooded areas, accounting for approximately 60% of the total influence on the variability of the flooded area [22]. In 2020, the worst drought recorded in sixty years happened, with an average annual precipitation 26% lower than the averages recorded from 1982 to 2020 [23]. In January 2020, 3506 fires were detected in the region, an increase of 302% compared to the averages recorded from the period of 2012–2019 for this same month [18]. In addition, the largest fire occurred in 2020, when flames destroyed almost one third of the biome [24], affecting a total of 3.9 million hectares [25,26] and emitting 115,576,561 tons of CO<sub>2</sub> into the atmosphere [18]. Recent estimates indicate that the fire had an indirect impact on 65 million vertebrates and 4 billion invertebrates, including threatened species such as *Panthera onca*, *Myrmecophaga tridactyla*, *Blastocerus dichotomus*, *Buteogallus coronatus*, and *Anodorhynchus hyacinthinus*. It also caused the alteration of habitat, shelter, and food for wildlife [27]. The main factors that contributed to this catastrophic scenario were the following: a severe drought that reduced water levels in the region, fires in the dry floodplain zone of the river, limitations to control brigade members, insufficient fire prevention strategies, changes in land use, and budget cuts [28].

The fires in the Pantanal are caused by anthropogenic activities derived from the opening of pasturelands for cattle [29], traditionally used to convert areas of natural vegetation into agricultural lands [30], and intensified by the impacts of climate change (longer drought periods) [31]. Fire dynamics are an important ecological factor for pastures and savannas, influencing the evolution of vegetation [32]. Fire management is the technical decision and action to avoid, preserve, control, or use fire in a given landscape. In turn, integrated fire management (IFM) fully considers ecological, cultural, and social approaches to managing fire [33]. Fire exclusion policies in protected areas have not produced the results desired by environmental agencies [1]. Their decisions have often led to severe fires due to the accumulation of combustible material [34], making it necessary to establish an IFM policy to prevent large-scale fire impacts, such as those that occurred in this biome in 2020. The results obtained in Brazil with the implementation of IFM since 2010 have reduced the area affected by fire and conflicts with communities, improving the interaction between biological diversity and human societies [35]. Prescribed burning (PB) is a technique commonly used to reduce the accumulated combustible material loads of fire-prone ecosystems worldwide [36,37]. It considers key aspects such as season, weather conditions, vegetation type and amount, and characteristics of combustible material [38]. PB is a controlled and intentionally ignited fire used for various purposes, such as reducing combustible material loads [39], managing invasive species [40], improving habitats, and promoting ecosystem health [41]. Evaluating PB using RPAS multispectral imagery allows the successful evaluation of soil and vegetation burn severity at very high spatial resolution

after PB [42]. High-resolution images from RPAS can be used to measure the effectiveness of prescribed burning and post-fire management actions [43]. In addition to determining impacts on vegetation [44] at a low cost with photogrammetric RPAS mapping at local scales [45]. It is necessary to understand the beneficial effect of fire on landscapes [46] so that proper management of combustible material can be established in the Pantanal [47], since fires can shape vegetation without altering its natural regime of protecting habitats and ecosystem services [48]. Although PBs have been used for predicting forest fires, our understanding of their effects on wetland ecosystems is still evolving and requires further research.

Satellite images are widely used to monitor the severity of fires and assess vegetation recovery processes [49]. The process considers variations in the reflectance levels of spectral signatures of the fire's effect on vegetation [50]. The use of unmanned aerial systems (UAS) provides higher spatial resolution compared to satellite imagery and manned aircraft, resulting in more accurate burn maps in terms of spatial detail [51]. Remote sensing techniques, including the use of a remotely piloted aircraft system (RPAS), offer a wide range of possibilities to detect and monitor fires, which may help to solve management problems and support near-real-time decision-making [52]. The use of RPAS for analyzing the dynamics of vegetation in wetland areas subjected to prescribed burnings has high potential in terms of spatial resolution, allowing us to determine how a fire may act as a regenerator of vegetation in certain fire-dependent ecosystems [53]. It also allows for rapid assessment of the ecological integrity of wetlands with multispectral imagery [54]. The use of multispectral sensors coupled with RPAS for fire management studies has also shown great potential compared to satellite mapping in terms of classification accuracy and spatial/spectral and temporal resolutions [51,55]. Spectral analysis allows us to obtain a spectral response of vegetation at different wavelengths [56], which can be used to estimate the severity of fires [57] based on the pre- and post-fire spectral response of the vegetation. Studies have demonstrated the effectiveness of visible and near-infrared (NIR) bands in forest fire detection and post-fire monitoring using different [58] airborne sensor platforms. This is a potential application of this equipment for the spatial analysis of burnings, and allows us to map fire-affected areas with precision, assessing their severity using geoprocessing techniques to detect different levels of intensity [59]. The results based on RPAS and spectral analysis contribute to a more complete understanding of fires, allowing more informed decision making and efficient planning of [60] PB actions. This study aims to evaluate the effect of PBs on three different macrohabitats within the SESC Pantanal Private Natural Heritage Reserve (Brazil) (M1: natural grassland flooded with a proliferation of *Combretum* spp., M2: natural grassland of seasonal swamps, and M3: natural grassland flooded with proliferation of *Vochysia divergens*) during three periods of the dry season (July, September, and October) in three analysis plots within each macrohabitat with PBs: early, mid, and late. Spectral and thermal analyses were conducted with data from a multispectral sensor coupled to an RPAS to generate data for the establishment of an integrated fire management in the Pantanal biome.

## 2. Materials and Methods

### 2.1. Study Area

The selected study area corresponds to areas of natural flooded fields that have undergone woody encroachment, resulting in a loss of biological diversity and reduction in native pasture productivity, affecting local livestock [61,62]. It is located in the Private Natural Heritage Reserve SESC Pantanal, at the geographic coordinates  $-16^{\circ}28'31''\text{N}$ ,  $-16^{\circ}51'50''\text{N}$ ,  $-56^{\circ}00'06''\text{W}$  and  $-56^{\circ}30'56''\text{W}$  in the municipality of Barão de Melgaço in the State of Mato Grosso, Brazil [63]. The total protected area is 107.996 hectares, corresponding to almost 1% of the total extension of the Mato Grosso Pantanal [64]. The climate in the reserve is typical savanna, of the "Aw" type according to the Köppen classification [65]. This area is characterized by floods that occur due to the overflow of the main rivers (Cuiabá and São Lourenço) and the relief slope in the plain. The phenomenon

is also affected by the rainfall regime that occurs with greater intensity from November to March, with an average annual rainfall between 1000 and 1500 mm, and by the low permeability of the soil horizons [66]. The evaluated macrohabitats (namely M1: natural grassland flooded with a proliferation of *Combretum* spp., M2: natural grassland of seasonal swamps, and M3: natural grassland flooded with a proliferation of *Vochysia divergens*) are representative of the reserve and show processes of woody encroachment, [67,68] (Figure 1). Each macrohabitat is composed of three PB analysis plots: early, mid, and late, corresponding to the months of July, September, and October 2021, respectively, periods defined as suggested by the Fire in the Cerrado Project [69,70].

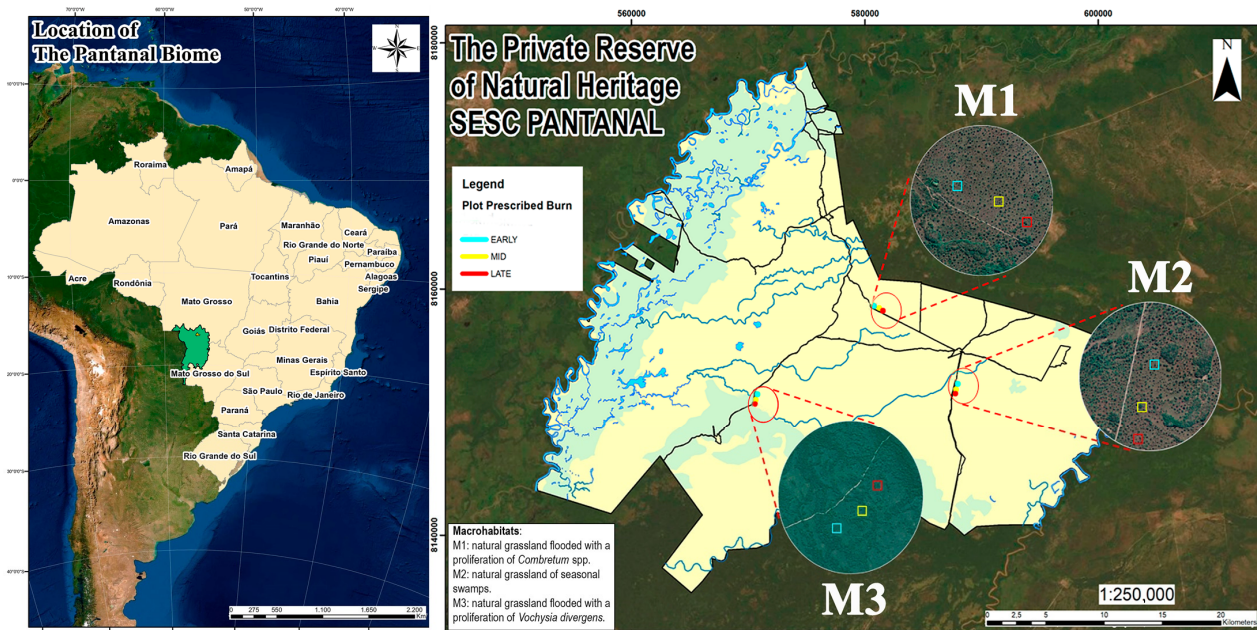


**Figure 1.** Location of the study area.

## 2.2. Data Acquisition

The data were collected using the MicaSense Altum sensor. It is a high-resolution multispectral camera equipped with six different sensors, five multispectral bands, and a long-wave thermal sensor (LWIR) that allows the collection of both multispectral and thermal data [71]. The camera has a built-in global positioning system (GPS) and a solar irradiance sensor (DLS 2.0) that records ambient light conditions and the angle of the sun for spectral calibration. The equipment was mounted on a DJI Matrice 100 RPAS. Table 1 shows the spectral/spatial resolution characteristics of the sensor and the location of the Altum camera's spectral bands (Figure S1).

Prior to the operation of the PBs, an aerial photogrammetric survey was carried out using an RPAS with a multispectral sensor attached. The early and mid burnings occurred on July 14, 15, and 16 and September 15, 16, and 17, respectively, while the late burnings occurred on October 26 and 27 2021 between 09:00 and 15:00. The post-fire flights took place one or two days after the PBs. The fieldwork for the PBs is described in the Supplementary Material.

**Table 1.** Multispectral sensor features.

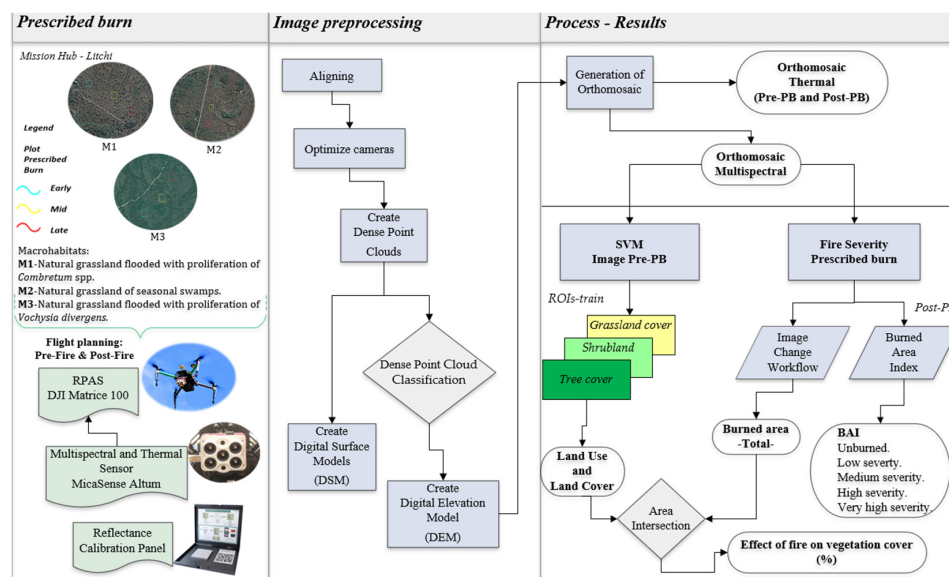
Band Name	Central	Bandwidth	Range	Sensor Resolution	GSD (Examples)
B1-Blue	475 nm	20 nm	443–507 nm	Multispectral: 3.45 $\mu$ m Pixel size; 2064 $\times$ 1544 px; 7.12 $\times$ 5.33 mm Sensor size 8 mm Focal length; 48° $\times$ 36.8° Field of view (h $\times$ v)	GSD-120 m (~400 ft) 5.2 cm (Multispectral) 81 cm (Thermal)
B2-Green	560 nm	20 nm	533–587 nm		
B3-Red	668 nm	10 nm	652–684 nm		
B4-Red Edge	717 nm	10 nm	705–729 nm	Thermal: 12 $\mu$ m Pixel size; 160 $\times$ 120 px; 1.92 $\times$ 1.44 mm Sensor size; 1.77 mm Focal length; 57° $\times$ 44.3° Field of view (h $\times$ v)	GSD-60 m (~200 ft) 2.6 cm (Multispectral) 41 cm (Thermal)
B5-NIR*	840 nm	40 nm	785–899 nm		
B6-LWIR*	11 $\mu$ m	6 $\mu$ m	5–17 $\mu$ m		

Nm: nanometer,  $\mu$ : micrometer, NIR\*: near-infrared, LWIR\*: long-wave infrared, GSD: ground sample distance.

### 2.3. Photogrammetric Processing

The images obtained from the sensor were processed using Agisoft Metashape version 1.7.5 and the Structure from Motion (SfM) and Scale-Invariant Feature Transform (SIFT) algorithms, allowing the generation of high-resolution spatial and radiometrically calibrated multispectral orthomosaic data. The processes in Metashape include (1) aligning images by calculating the position and orientation of cameras and detecting matching key points between images, (2) generating a dense point cloud using depth maps calculated from stereo matching, (3) classifying the dense point cloud to separate ground points, (4) building a digital elevation model (DEM), and (5) generating the orthomosaic. Finally, the orthomosaics were exported for each plot in GeoTIFF file format using the EPSG Sirgas 2000 21S datum. The real reflectance values were obtained by dividing each band by 32,768 to obtain normalized values within the range 0 to 1. For the thermal images, the LWIR thermal band calibration was used ( $= (B6/100) - 275.13$ ).

The reprojection function was used on all post-PB images using ArcGIS 10.8 software. Subsequently, metadata calibration was performed on the orthomosaics generated from the six independent spectral bands captured by the MicaSense Altum sensor: blue 475 nm (B4), green 560 nm (B5), red 668 nm (B6), red edge 717 nm (B7), near infrared 840 nm (B8), and thermal 11  $\mu$ m (B9) [72], as well as their respective wavelengths. The equipment used, parameters for conducting flights, photogrammetric processing to obtain thermal and multispectral orthomosaic products, supervised classification of pre-PB coverage, and classification of fire severity were examined through respective analyses to determine their effects on each macrohabitat. Figure 2 presents the data.

**Figure 2.** Flowchart of procedures performed in the study.

#### 2.4. Supervised Classification

The support vector machine (SVM) was used for data classification according to the method in [73]. It is a reliable and effective machine learning algorithm for the classification process of multispectral aerial images. Classification is the process through which the algorithm is trained to identify different types of ground cover using training samples and regions of interest (ROIs), which are specific areas of the image used as training samples in supervised classification [74]. This study used SVM to identify pixel variability in determining three classes: grass cover (1), shrub cover (2), and tree cover (3) for pre-fire images and determine the effect of PB on each type of cover in post-fire images. The ROIs-train were created by selecting pixels with a random sampling, with a size of  $2 \times 2$  pixels, choosing a total of 20 pixels for each class distributed over the entire area of each plot.

The evaluation of the classification for the different periods of PB was by means of accuracy indexes and verification during field tasks, validating the three types of physiology of each plot (pre-fire condition before PB). To test the accuracy, 10 sites of each class were sampled (ROIs-truth) from the images processed using visual analysis according to the criteria in [75], considering them as true fields to establish unbiased results of the analyses and not sampling the same sites used as references for the classification (ROIs-train). The construction of a confusion matrix covering the following parameters was performed: kappa index, overall accuracy. The evaluation of classification quality was based on the following kappa index ranges: poor ( $<0.20$ ), acceptable ( $0.20-0.40$ ), good ( $0.41-0.60$ ), very good ( $0.61-0.80$ ), and excellent ( $0.81-1.00$ ), as established in [76].

#### 2.5. Fire Severity

Monitoring based on electromagnetic spectrum regions, infrared, and thermal regions allows for a detailed discrimination and quantification of fire severity and temperature levels, as observed using the MicaSense Altum sensor [75]. To calculate the burned area, the “Image change workflow” tool in ENVI 5.3 was used. It compares two images of the same geographic extent taken at different times. It identifies differences between them. The difference can be computed for a specified on a feature index. It uses the Normalized Difference Vegetation Index (NDVI) of pre- and post-fire images as a reference. The initial input images (pre-PB) and post-input (post-PB) were taken to obtain the output of the area where the mute value, in this case affected by the fire, indicates the area where there is a decrease in vegetation coverage [76]. This process geometrically aligns two images with different viewing geometry and/or different terrain distortions into the same coordinate system. This registration identifies and establishes common joining points through reprojection with a first-order polynomial deformation for change determination and burned area determination.

Similarly, the Burned Area Index (BAI) presented by [77] was specifically used for the discrimination of burned zones in the red and near-infrared spectral domains, providing a high discrimination capacity compared to other burning indices. Table 2 shows the spectral indices used. The BAI allows for separating and determining the area affected by fires during the three periods of analysis according to the classification pattern presented in [59,78,79]. For this purpose, there were five classification levels: non-burned area (1), low-severity burn (2), medium-severity burn (3), high-severity burn (4), and very high-severity burn (5). The areas of the plots were verified after burning was performed during fieldwork PBs.

**Table 2.** Spectral index.

Index Spectral	Formula	Reference
Normalized Difference Vegetation Index (NDVI)	$\frac{(\rho_{NIR} - \rho_{Red})}{(\rho_{NIR} + \rho_{Red})}$	[50]
Burned Area Index (BAI)	$\frac{1}{(0.1 - \rho_{Red})^2 + (0.06 - \rho_{NIR})^2}$	[77]

Note:  $\rho_{NIR}$ : near-infrared band and  $\rho_{Red}$ : red band.

### 3. Results

#### 3.1. Land Use and Land Cover

In general terms, the pre-fire supervised classification using the SVM algorithm indicates that the predominant vegetation in all macrohabitats is of the grassland type, except in M3, which is more heterogeneous and presents a proliferation of *V. divergens* with a higher percentage of trees and shrubs compared to the other two macrohabitats (Figure 3). The light fuel material is pasture and the heavy fuel material is woody vegetation in all plots. The predominant cover of M1 and M2 is of the grassland type: over 73% in each study plot, which is because they are macrohabitats of clean natural grasslands, the first with a degree of proliferation of *Combretum* spp. and the second of seasonal swamps. Table 3 shows the spatial distribution and differences in the three types of coverage in each PB plot of the macrohabitats.

**Table 3.** Percentage of each macrohabitat covered by vegetation growth form present before PBs.

Macrohabitat PB Plot	Macrohabitat 1			Macrohabitat 2			Macrohabitat 3		
	Early	Mid	Late	Early	Mid	Late	Early	Mid	Late
Tree cover	11.46	11.38	5.55	8.84	8.90	14.51	21.91	14.62	44.30
Shrubland	12.88	8.84	14.76	1.91	18.68	6.42	22.84	25.44	35.04
Grassland	76.36	80.48	80.14	90.06	73.17	79.87	56.06	60.64	25.20

The accuracy of the overall index showed values above 80% for the years studied, with the lowest value occurred in M3-Early (90.66%) and the highest (97.54%) in M2-Mid. The kappa index showed values above 0.89, indicating excellent performance for the classification of all analysis plots, and a substantial agreement between the classification and the values presents in the field. Table 4 shows the different overall accuracy values and kappa coefficient for each plot.

**Table 4.** Overall accuracy and kappa coefficient of land use and land cover classification for each PB.

Macrohabitat	PB Plot	Overall Accuracy		Kappa Coefficient
		Pixels	Percent	
M1: natural grassland flooded with a proliferation of <i>Combretum</i> spp.	Early	(77,884/79,121)	93.38%	0.9236
	Mid	(190,632/195,989)	97.27%	0.9228
	Late	(317,114/329,808)	96.15%	0.9617
M2: natural grassland of seasonal swamps	Early	(98,788/100,910)	95.92%	0.9163
	Mid	(108,235/110,961)	97.54%	0.8905
	Late	(274,823/283,666)	96.88%	0.9036
M3: natural grassland flooded with proliferation of <i>Vochysia divergens</i>	Early	(10,393/112,356)	90.66%	0.9533
	Mid	(101,010/105,009)	96.19%	0.9376
	Late	(150,842/162,692)	94.28%	0.9152

The orthomosaics produced allow an easy observation of the area affected by PBs for each analyzed plot (Figure 4). They show the before (pre-fire) and after (post-fire) for each event. The obtained resolution scale is 5.4 cm/pixel ground sampling distance (GSD). In them, it is possible to clearly distinguish three land use and land cover classes mapped in the Pantanal landscape, with natural formations of grasslands and seasonal flooding areas of macrohabitats, and the different firebreaks and plot delimitations.



Figure 3. Natural cover within the analysis plots for each period of PB evaluated.

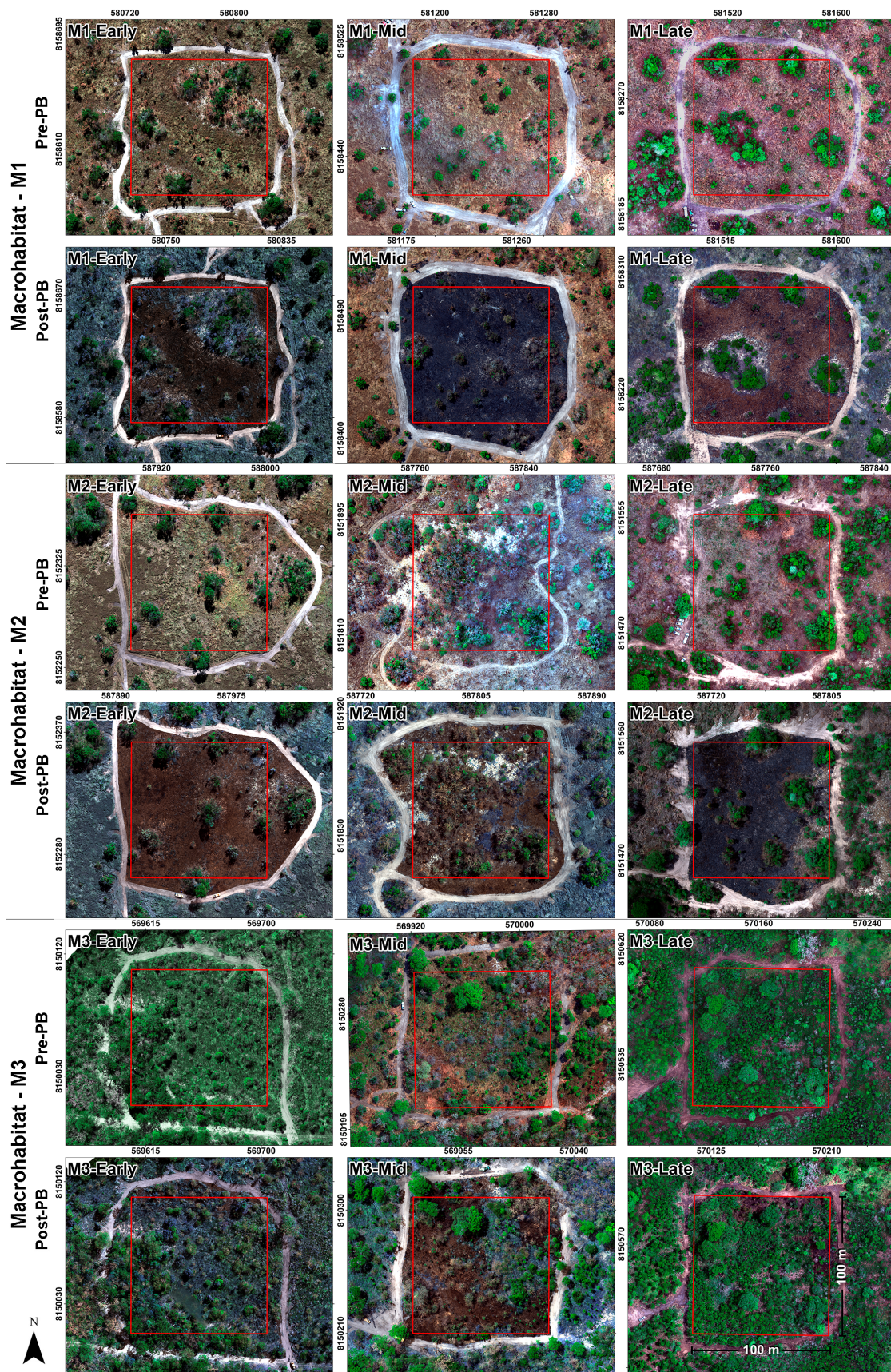
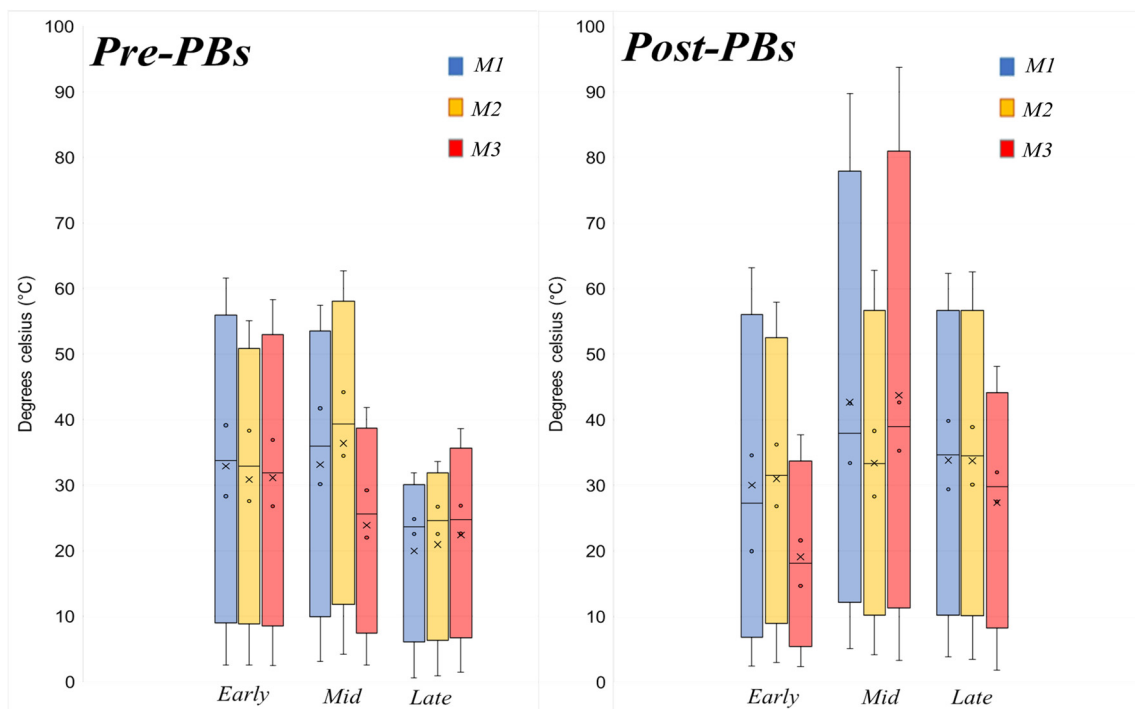


Figure 4. Orthomosaics of the three PB periods of each macrohabitat evaluated.

### 3.2. Thermal Sensor Behavior

The box plot shows the sensor's thermal variation (Figure 5). Prior to the various disturbances, the average temperature for the PBs ranged from 24.8 to 39.13 °C, showing a more stable level in July and variation for the other two burning periods. In the case of post-fire events, the average temperature ranged from 21.61 to 39.82 °C. The highest recorded temperature was for the mid burning plot (September) in M3, which was 94.29 °C, and the lowest was 19.97 °C for the early burning plot (July) in the same M3.



**Figure 5.** Pre-PBs and post-PBs, thermal band behavior.

The thermal band behavior of the sensor shows a remarkable differentiation in terms of temperature levels in the prescribed burning events carried out one or two days after the passage of the fire. Figure 6 shows the spatial behavior of temperature levels in °C obtained during the flights. Red colors indicate higher temperatures and green colors indicate lower temperatures. This spatial temperature behavior correlates directly with the burned area of the plot. In areas with a greater presence of tree specimens, they generate a lower temperature at the site where they are (due to the difference in combustible material conditions of each growth form), while grassy areas show the highest level of variation post-fire events.

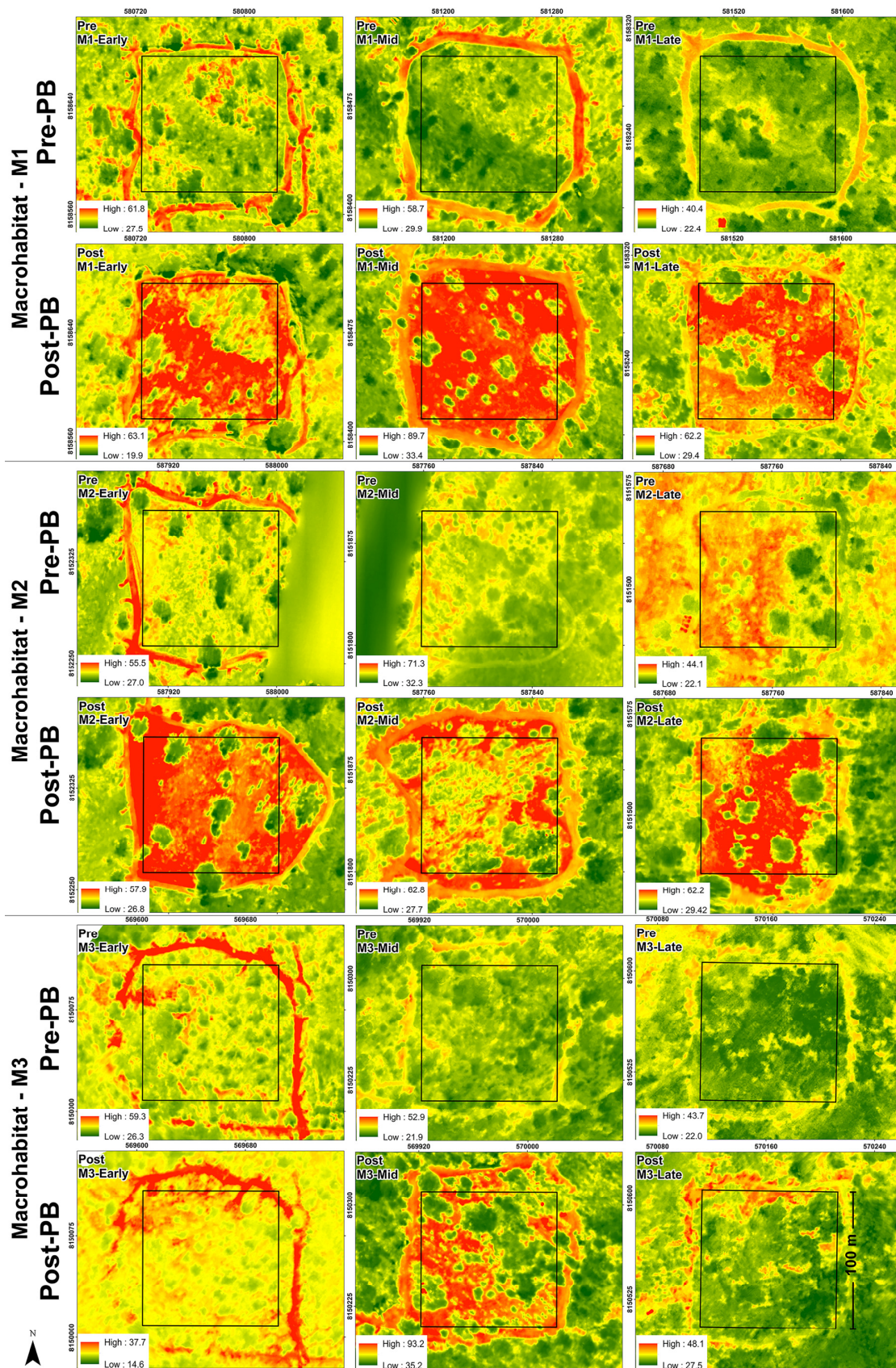


Figure 6. Pre-PB and post-PB thermal band spatial behavior.

### 3.3. Climatological Variables in the Prescribed Burning Moment

The climatological variables acquired in the field correspond to the data Table 5 shows. Data were environmental conditions during the execution of the OPs for each plot according to the burning period. The average wind speed ranged from 0.7 to 3.3 km/h. As a parameter for performing the PB, burnings were carried out against the wind direction, and the wind presented different directions for each disturbance. Similarly, the behavior of the relative humidity of the environment presented high variation between burning periods and plots, but stable behavior during the execution of the burning for each plot. The values obtained were 38.8% for the mid burning plot of M1, which was the lowest humidity in relation to the behavior presented by the same macrohabitat but evaluated in the late burning period, which was 76.5%, the highest recorded.

**Table 5.** Climatological variables before PBs.

Rain	Variable	M1—PB Early	M2—PB Early	M3—PB Early
30 days without rain	Wind speed (km/h)	0.7	2.7	0.8
	Temperature (°C)	31	35.4	36.2
	Relative air humidity (%)	54.7	38.6	40.6
Rain	Variable	M1—PB Mid	M2—PB Mid	M3—PB Mid
5 to 10 days without rain	Wind speed (km/h)	1.9	1.3	2.5
	Temperature (°C)	40	36.6	40.1
	Relative air humidity (%)	38.8	48.3	43.6
Rain	Variable	M1—PB Late	M2—PB Late	M3—PB Late
Less than 1 day without rain	Wind speed (km/h)	1.6	3.3	0.7
	Temperature (°C)	29.7	29.6	35.1
	Relative air humidity (%)	76.5	69.8	60.5

Note: The data correspond to average data for each parameter collected during the PBs.

On the other hand, the temperature can be correlated with the behavior of the thermal band presented in Figure 6 and the data in Table 5. In September, the recorded temperatures reached average maximum values of 40 °C, 36.6 °C, and 40.1 °C for each parcel of macrohabitats in this burning period. In contrast, M3, despite recording higher ambient temperatures for all three PB events, suffered a lesser effect from the passage of fire compared to the other two areas of analysis. This is directly associated with the type of macrohabitat (natural flooded grassland with proliferation of *V. divergens*). For October, less than one day had no rain before performing the PBs. This directly affected the behavior of the fire associated with the types of vegetation cover formation, where there was a higher number or presence of tree specimens, and the effect of the passage of fire was smaller.

### 3.4. Effects of Burning on Vegetation Cover

The burned area within each macrohabitat and plot is shown in Figure 7 ('Effect of burning on study macrohabitats'). It indicates the total burned area for each vegetation type. The plot that showed the highest degree of burning corresponded to the macrohabitat M2 during the early PB, with a total burned area of 86.79%, mainly comprising the burning of the grassland cover (83.14%), which was also the highest burned value recorded for this type of cover in all analyzed plots. The arboreal cover had a lower effect of fires compared to the other two vegetation classes, which presented an effect no higher than 5.95%. In turn, the highest effect of fire on the arboreal cover was directly associated with the macrohabitat, with a higher number of tree specimens present in M3, and the mid burning plot of this macrohabitat showing an effect of 8.37% for this type of cover, achieving the objective of PB by reducing the light fuel material composed of grasses and pastures and causing a low impact on the arboreal cover. The macrohabitats show distinct linear behavior with respect to the BP period. While M1 and M2 show an overall decrease in burned area over time, M3 does not follow a clear linear decreasing trend. In the case of M2, although the increase in

the final period may indicate a greater effect of burning, the overall trend is still a decrease in burned area.

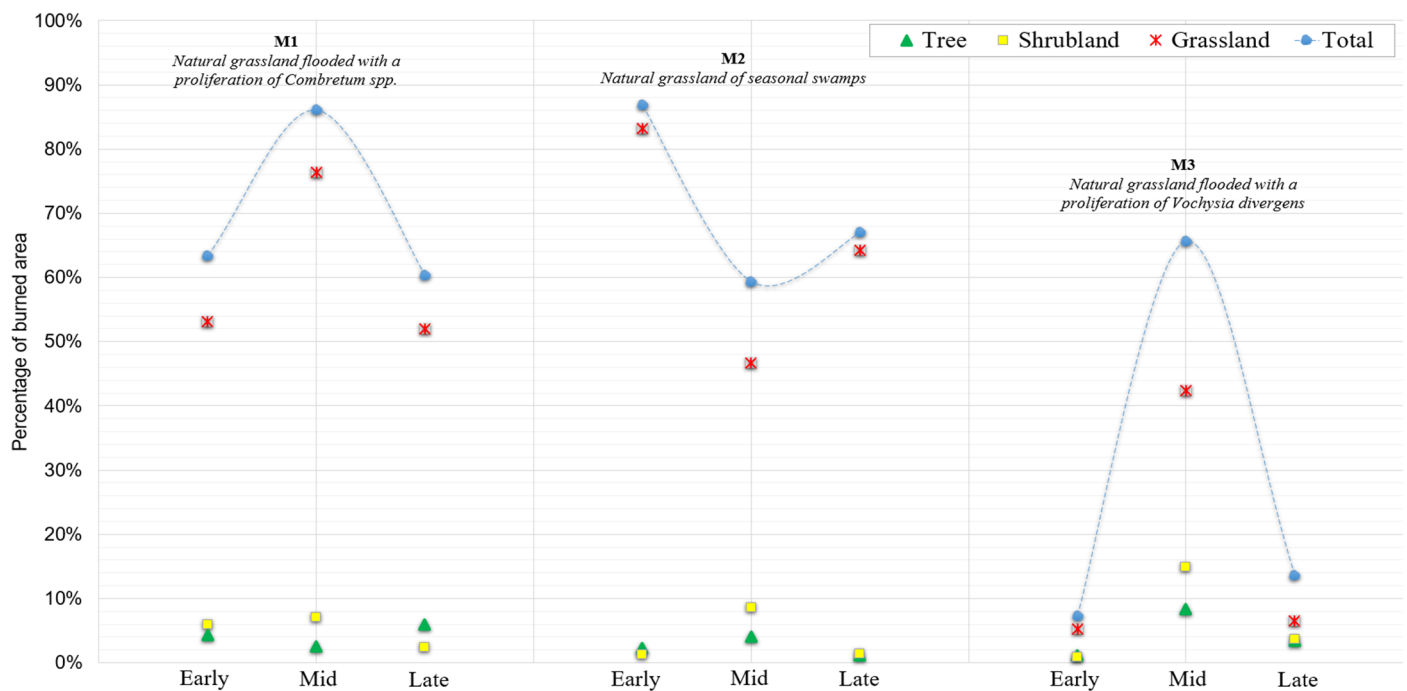


**Figure 7.** Effect of burning on study macrohabitats.

### 3.5. Severity of PBs

The severity degree of the burnings is presented in Figure 8. Green colors indicate unburned areas and red colors indicate areas with high burn severity. M3 had a lower degree of alteration due to fire, with percentages of unburned area of 64.83% and 88.97% for the early and late PBs, respectively. The September events showed a similar behavior for the three different macrohabitats compared to the other two periods of PBs. The early plot of M2 recorded the highest area burned, revealing that the unburned area was only 0.55%. On the other hand, the early PB plot of M1 had the highest burn severity, with 20.23% of its total area. Figure 9 shows the percentage of the effect of different levels of fire severity associated with BAI for the three vegetation covers in the analysis plots presented in Table S1.

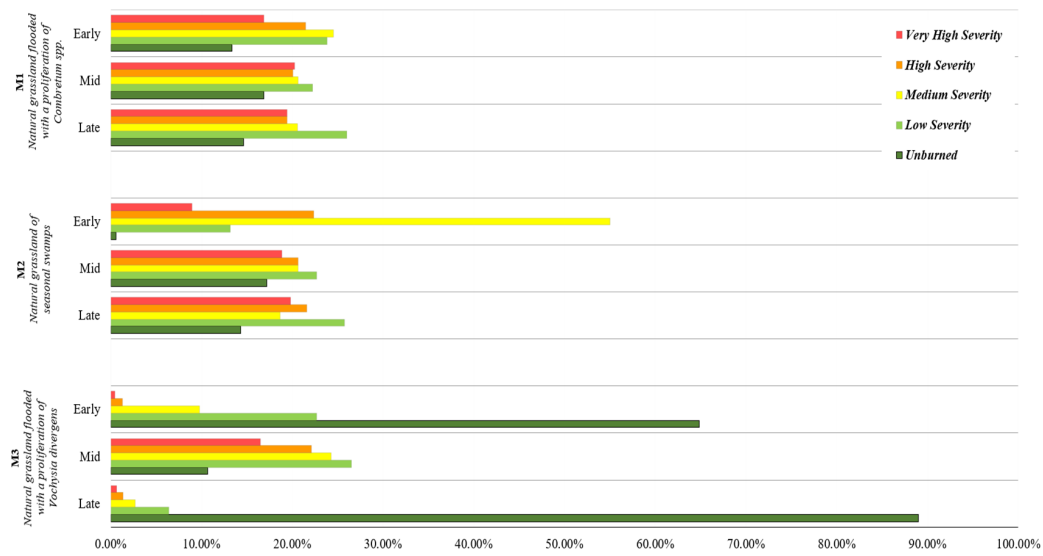


Figure 8. Fire severity—BAI in each macrohabitat and the evaluated period of PBs.

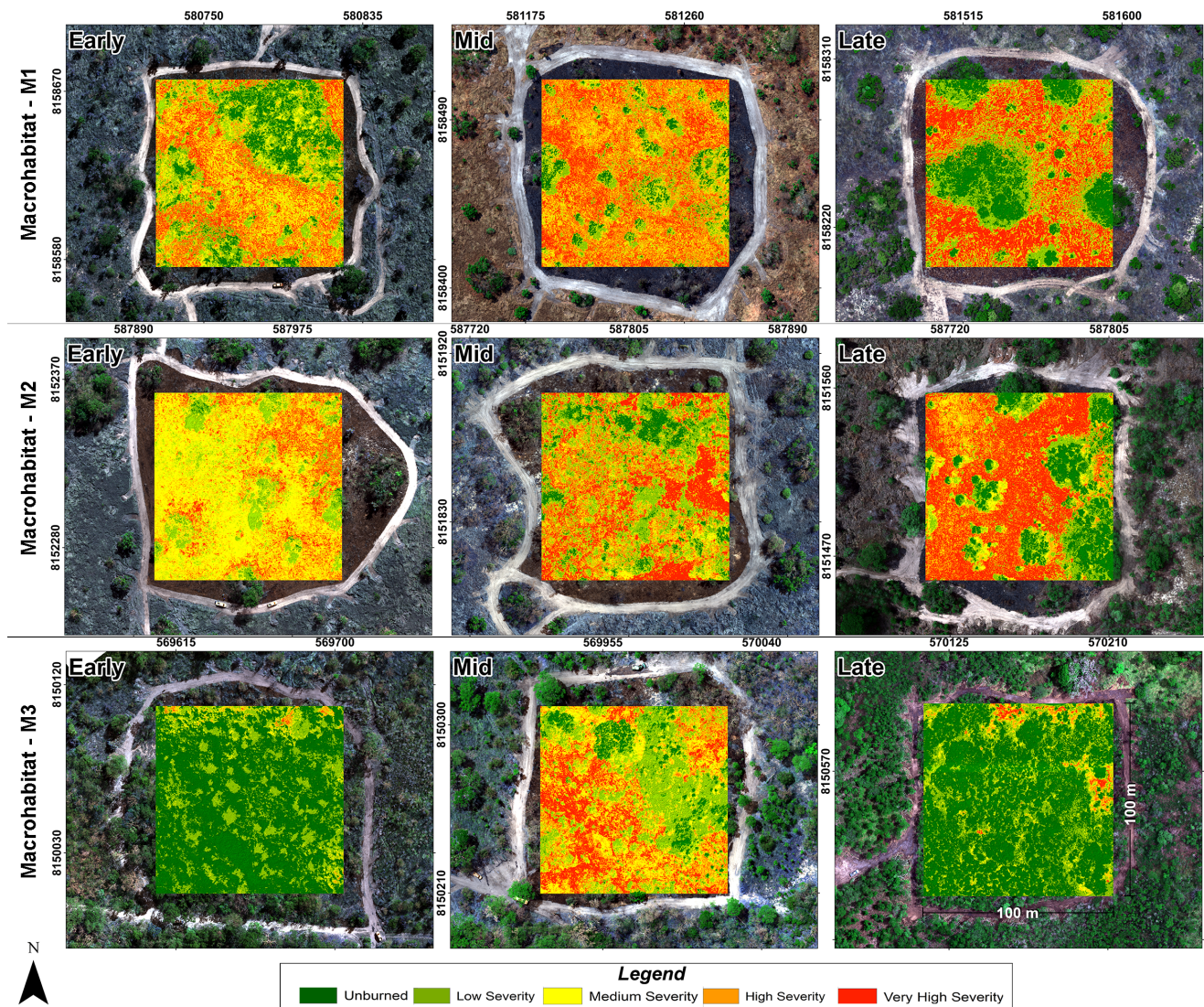


Figure 9. PBs severity—BAI.

#### 4. Discussion

The results of this study contribute to determining the effect of prescribed fires as a way to prevent large wildfires in three different types of macrohabitats in the Pantanal biome. Studies have shown the importance of remote sensing as a fire management tool in conservation units [80]. They can establish priority areas for IFM [14] and constitute an important management input within the SESC Pantanal Private Natural Heritage Reserve. Remote sensing is an alternative method to evaluate and characterize the effects of fires [81], and the use of RPAS allows us to obtain high-detail images in spatial resolution, generating new perspectives in terms of spatial and temporal resolution [55]. In our study, we obtained a high level of detail (GSD 5.4 cm/pixel), allowing us to evaluate the effects of fires on vegetation and measure the efficacy of prescribed fires, showing the applicability of multispectral data obtained using RPAS for fire damage analysis [42]. The effect of different prescribed fires on the types of vegetation cover determined using the SVM algorithm indicates an adequate differentiation in the three types of cover identified in our analysis plots, showing a suitable spectral separation of classes [82]. The kappa index shows that the SVM classification algorithm presents a high degree of accuracy and allows a clear understanding in terms of differentiating vegetation phytophysiognomies [83]. According to our kappa statistic values, the classification performance level in the current study can be classed as excellent [84]. The Altum camera allows the correct identification of plots and plant phenotypes [85].

Thermal analysis in the mid-infrared and thermal domains, including the mid-infrared (MIR: 2.5–8  $\mu\text{m}$ ) and thermal infrared (TIR: 8–14  $\mu\text{m}$ ) bands [86], allows us to determine the water stress plants are subjected to. This spatial behavior reflected in grassland covers, which have the highest level of variation for post-fire events in PBs, thus demonstrated that different forms of plant growth, such as grass, shrubs, and trees, presented varying levels of flammability, as well as revealing the dominant role that grasslands have as drivers of flammability in tropical savannas [87] by being the cover that is most affected by fire. Burned areas are also related to the continuity of fine combustible material and wind, where natural grassland flooded with a proliferation of *Combretum* spp. and seasonal bog natural fields are prone to fire, but with adapted ecological characteristics [88] compared to natural flooded fields with proliferation of *V. divergens*. The spatial pattern has a higher tree density, providing protection of plots against wind, thus igniting the combustible material process at a slower pace [89,90].

These differences in the effects of burning on vegetation cover can be attributed to factors such as vegetation composition and fire resistance. Climatic variables, microclimate, fuel quantity, and fuel type contribute to vegetation flammability [91]. The results suggest that in the macrohabitats evaluated here, the severity of burning is more related to the period without rain (periods of more than ten days without rain (PB-mid) and 30 days without rain (PB-early)) than to air humidity and temperature. Studies such as [92] report that the use of PB in tropical areas occurs at the beginning of the dry season, resulting in less severe forest fires. In Brazil, fire management occurs at the beginning, middle, and end of the dry season [69]. Our PBs were conducted during three periods of the dry season: in July, September, and October. However, it was an atypical year in terms of rainfall patterns. We based our information on historical data from two meteorological stations (Poconé and Barrão de Melgaço) of the Brazilian National Water Agency (ANA) ([www.snirh.gov.br/hidroweb/serieshistoricas](http://www.snirh.gov.br/hidroweb/serieshistoricas) (accessed on 20 January 2023)) (Figure S11), close to the study area. The data correlate with what happened in 2020, where irregular weather patterns could generate large forest fires [93]. Weather conditions are important for understanding fire behavior in a prescribed burn. Wind speed can affect [89,90] fire spread, while temperature and relative humidity can influence the intensity and severity of burns [87]. It is vitally important to consider these meteorological factors when planning and executing prescribed burning, ensuring the safety and effectiveness of fire management actions [88–90].

In the Pantanal biome, natural flooding processes and fire may affect the structure of vegetation in seasonal wetlands [94]. In general, the greatest effect of fire occurs on the coverage of grass species and the layer of combustible material close to the surface [95]. Grass is the fuel that is most rapidly incinerated. PBs contribute to reducing the fine combustible material in the area, as this coverage presents higher rates of propagation and intensity compared to forested areas [96]. The homogenization in the Pantanal biome is mainly due to activities resulting from changes in land use, namely the opening of vegetation for pastures and agricultural areas, making the territories more homogeneous and potentially intensifying fires [31,97]. Homogeneous areas will be more affected by fire than heterogeneous areas, where the impact of fire is lower (M3). On the other hand, the process of woody invasion is a major problem in the Pantanal [61], homogenizing the landscape and resulting in the reduction in grassland areas, causing a loss of diversity due to the monodominance of aggressive plants such as *Combretum laxum* Jacq. [98] and *V. divergens*, associated with the flood cycle in the Pantanal [62]. They are present in the evaluated macrohabitats M1 and M2. Therefore, PBs in these areas can act as a renewing agent for native vegetation and as an inhibitor of invasive vegetation [53], achieving the objectives of fire management in protected areas by generating heterogeneous mosaics of the landscape for the protection of biodiversity [99].

The BAI used to determine the effect of fires on vegetation shows suitability for detecting post-fire burned areas, taking advantage of the visible (B3) and NIR spectral characteristics and making clear the observation of the spatial pattern of fire behavior, as well as its severity level, mainly associated with grassland cover. This spectral index and the NDVI in tropical wetlands allow an adequate discrimination of fire-damaged surfaces [100]. The use of a multispectral sensor makes it easier to record high-precision, rapid, and indirect measurements based on the vegetation spectral response [101]. The spectral behavior of the severity of burnings indicates a low level of impact on tree covers, as observed in the electromagnetic spectrum reflectance response [102]. The severity of the burnings may affect vegetation recovery [103], being low in the upper covers and eliminating the combustible material present in the plots of the M1 and M2 macrohabitats and the PB-mid plot of M3.

## 5. Conclusions

There is no single fire management strategy for the entire Pantanal biome. It must be addressed integrally [104] according to the type of fuel material, phytophysiology, climatic conditions, and duration of flooding at the landscape scale and considering the different macrohabitats of this ecosystem associated with cultural and economic uses and involving different stakeholders in their management [105]. This study contributes to the understanding of the effects of PB as a preventive measure against large forest fires in three different macrohabitats of the Pantanal. Spectral analysis allows obtaining the true response of vegetation pre- and post-fire. It also shows the severity level of the fire's passage over the vegetation. The use of RPAS data provides information with high detail. The overall classification accuracy was high, with values above 80%, indicating reliable model performance. Early burning periods (PB-early) are the best option and can meet management objectives. Mid burning periods (PB-mid) are also good options, but they require a higher degree of experience on the part of firefighters and more inputs. The results revealed that PBs had a varied impact on the different vegetation cover types, demonstrating that PBs were effective in terms of reducing combustible material in grassland areas while minimizing the impact on tree cover. By implementing PBs, it is possible to increase ecological niches by generating heterogeneity within the landscape in fire-adapted ecosystems, presenting good results in terms of reducing accumulated fuel material composed mainly of pastures and functioning as a measure of protection against and prevention of fires. It is necessary to plot a map of biomass refills of combustible materials for the Pantanal biome to allow adequate planning and implementation of PBs [106]. The cost–benefits of implementing IFM may

reduce the costs of burned areas by 50% [107]. Currently, the management approach based on IFM allows a reduction in large-scale forest fires [108].

**Supplementary Materials:** The following supporting information can be downloaded at: <https://www.mdpi.com/article/10.3390/rs15112934/s1>, Figure S1: Attribute description of the features and electromagnetic spectrum of the MicaSense Altum multispectral sensor and RPAS; Figure S2: Flight planning; Figure S3: Drone calibration; Figure S4: Recognition of plant physiognomies; Figure S5: Pre-burn flight; Figure S6: Prescribed Burn; Figure S7: PBs in the experimental macrohabitats; Figure S8: Fire control; Figure S9: Post-fire flight; Figure S10: Burn verification; Figure S11: Pattern of precipitation regime in the region; Table S1. Percentage PBs severity. Reference [109] is cited in the supplementary materials.

**Author Contributions:** Conceptualization: H.E.P.V., G.M.N., C.N.B., L.G.G. and G.H.P.d.M.R.; methodology: H.E.P.V. and G.M.N.; software: H.E.P.V. and G.M.N.; validation: H.E.P.V., G.M.N., C.N.B., L.G.G. and G.H.P.d.M.R.; formal analysis: H.E.P.V., G.M.N., C.N.B. and G.H.P.d.M.R.; investigation: H.E.P.V., G.M.N., C.N.B., L.G.G. and G.H.P.d.M.R.; resources: G.M.N., C.N.B. and L.G.G.; data curation: H.E.P.V. and G.M.N.; writing—original draft preparation H.E.P.V., G.M.N., C.N.B. and G.H.P.d.M.R.; writing—review and editing: H.E.P.V., G.M.N., C.N.B., L.G.G. and G.H.P.d.M.R.; visualization: H.E.P.V., G.M.N., C.N.B., L.G.G. and G.H.P.d.M.R.; supervision: G.M.N., C.N.B. and G.H.P.d.M.R.; project administration: C.N.B., G.M.N. and L.G.G.; funding acquisition: C.N.B., G.M.N. and L.G.G. All authors have read and agreed to the published version of the manuscript.

**Funding:** This work was supported by the project “Assessment of the effect of fire on biodiversity and soil, contributions to the establishment of Integrated Fire Management in the Pantanal” (Edital N°012/2020 SEMA—MIF PANTANAL. The Ministry of Science and Technology provided financial support to the Pantanal Research Network (grant number: FINEP 01.20.0201.00). The first author received a scholarship from the Organization of American States (OAS) and the Group of International Cooperation of Brazilian Universities (GCUB), with the support of the Division of Educational Issues of the Ministry of External Relations of Brazil (DTED/MRE), in the framework of the Program of Alliances for Education and Training of the OAE (PAEC OAS-GCUB), from the call for proposals of the OAS-GCUB program number 001/2020.

**Data Availability Statement:** Not applicable.

**Acknowledgments:** The authors thank the Instituto Chico Mendes de Biodiversidade (ICMBio), the Private Reserve of Natural Heritage SESC Pantanal, firefighters from the Mato Grosso State Fire Brigade, and LabSensoR/-Universidade Federal de Mato Grosso (UFMT) for the field support and equipment used.

**Conflicts of Interest:** The authors declare no conflict of interest.

## References

- Durigan, G. Zero-Fire: Not Possible nor Desirable in the Cerrado of Brazil. *Flora* **2020**, *268*, 151612. [CrossRef]
- Bowman, D.M.J.S.; Balch, J.K.; Artaxo, P.; Bond, W.J.; Carlson, J.M.; Cochrane, M.A.; D’Antonio, C.M.; DeFries, R.S.; Doyle, J.C.; Harrison, S.P.; et al. Fire in the Earth System. *Science* **2009**, *324*, 481–484. [CrossRef]
- Pausas, J.G. Evolutionary Fire Ecology: Lessons Learned from Pines. *Trends Plant Sci.* **2015**, *20*, 318–324. [CrossRef] [PubMed]
- Hardesty, J.L.; Myers, R.; Fulks, W. Fire, Ecosystems, and People: A Preliminary Assessment of Fire as a Global Conservation Issue. *Fire Manag.* **2005**, *22*, 78–87.
- Balch, J.K.; Schoennagel, T.; Williams, A.P.; Abatzoglou, J.T.; Cattau, M.E.; Mietkiewicz, N.P.; Denis, L.A.S. Switching on the Big Burn of 2017. *Fire* **2018**, *1*, 17. [CrossRef]
- Fidelis, A.; Alvarado, S.T.; Barradas, A.C.S.; Pivello, V.R. The Year 2017: Megafires and Management in the Cerrado. *Fire* **2018**, *1*, 49. [CrossRef]
- He, T.; Lamont, B.B.; Pausas, J.G. Fire as a Key Driver of Earth’s Biodiversity. *Biol. Rev.* **2019**, *94*, 1983–2010. [CrossRef]
- Pausas, J.G. Generalized Fire Response Strategies in Plants and Animals. *Oikos* **2019**, *128*, 147–153. [CrossRef]
- Enright, N.; Fontaine, J.B.; Bowman, D.M.J.S.; Bradstock, R.A.; Williams, R.J. Interval Squeeze: Altered Fire Regimes and Demographic Responses Interact to Threaten Woody Species Persistence as Climate Changes. *Front. Ecol. Environ.* **2015**, *13*, 265–272. [CrossRef]
- Rossetti, I.; Cogoni, D.; Calderisi, G.; Fenu, G. Short-Term Effects and Vegetation Response after a Megafire in a Mediterranean Area. *Land* **2022**, *11*, 2328. [CrossRef]
- Gutowski, J.M.; Sućko, K.; Borowski, J.; Kubisz, D.; Mazur, M.A.; Melke, A.; Mokrzycki, T.; Plewa, R.; Żmihorski, M. Post-Fire Beetle Succession in a Biodiversity Hotspot: Białowieża Primeval Forest. *For. Ecol. Manag.* **2020**, *461*, 117893. [CrossRef]

12. Marriner, N. Fire in Mediterranean Ecosystems: Ecology, Evolution and Management. *Méditerranée* **2013**, *111*. [[CrossRef](#)]
13. Jones, G.M.; Tingley, M.W. Pyrodiversity and Biodiversity: A History, Synthesis, and Outlook. *Divers. Distrib.* **2022**, *28*, 386–403. [[CrossRef](#)]
14. Schmidt, I.B.; Fonseca, C.B.; Ferreira, M.C.; Sato, M.N. Experiências Internacionais de Manejo Integrado Do Fogo Em Áreas Protegidas—Recomendações Para Implementação de Manejo Integrado de Fogo No Cerrado. *Biodivers. Bras.* **2016**, *6*, 41–54. [[CrossRef](#)]
15. Pivello, V.R.; Vieira, I.; Christianini, A.V.; Ribeiro, D.B.; da Silva Menezes, L.; Berlinck, C.N.; Melo, F.P.L.; Marengo, J.A.; Tornquist, C.G.; Tomas, W.M.; et al. Understanding Brazil's Catastrophic Fires: Causes, Consequences and Policy Needed to Prevent Future Tragedies. *Perspect Ecol. Conserv.* **2021**, *19*, 233–255. [[CrossRef](#)]
16. Berlinck, C.N.; Batista, E.K.L. Good Fire, Bad Fire: It Depends on Who Burns. *Flora* **2020**, *268*, 151610. [[CrossRef](#)]
17. Oliveira, M.T.d.; Damasceno-Junior, G.A.; Pott, A.; Paranhos Filho, A.C.; Suarez, Y.R.; Parolin, P. Regeneration of Riparian Forests of the Brazilian Pantanal under Flood and Fire Influence. *For. Ecol. Manag.* **2014**, *331*, 256–263. [[CrossRef](#)]
18. Pletsch, M.A.J.S.; Silva Junior, C.H.L.; Penha, T.V.; Körting, T.S.; Silva, M.E.S.; Pereira, G.; Anderson, L.O.; Aragão, L.E.O.C. The 2020 Brazilian Pantanal Fires. *Acad Bras. Cienc.* **2021**, *93*, 20210077. [[CrossRef](#)]
19. Silva, J.B.; Valle Junior, L.C.G.; Faria, T.O.; Marques, J.B.; Dalmagro, H.J.; Nogueira, J.S.; Vourlitis, G.L.; Rodrigues, T.R. Temporal Variability in Evapotranspiration and Energy Partitioning over a Seasonally Flooded Scrub Forest of the Brazilian Pantanal. *Agric. For. Meteorol.* **2021**, *308–309*, 108559. [[CrossRef](#)]
20. Junk, W.J.; Nunes, C. Pantanal: A Large South American Wetland at a Crossroads. *Ecol. Eng.* **2005**, *24*, 391–401. [[CrossRef](#)]
21. Manrique-Pineda, D.A.; de Souza, E.B.; Paranhos Filho, A.C.; Cáceres Encina, C.C.; Damasceno-Junior, G.A. Fire, Flood and Monodominance of *Tabebuia Aurea* in Pantanal. *For. Ecol. Manag.* **2021**, *479*, 118599. [[CrossRef](#)]
22. Pereira, G.; Ramos, R.d.C.; Rocha, L.C.; Brunzell, N.A.; Merino, E.R.; Mataveli, G.A.V.; Cardozo, F.d.S. Rainfall Patterns and Geomorphological Controls Driving Inundation Frequency in Tropical Wetlands: How Does the Pantanal Flood? *Prog. Phys. Geogr. Earth Environ.* **2021**, *45*, 669–686. [[CrossRef](#)]
23. Mataveli, G.A.V.; Pereira, G.; de Oliveira, G.; Seixas, H.T.; Cardozo, F.d.S.; Shimabukuro, Y.E.; Kawakubo, F.S.; Brunzell, N.A. 2020 Pantanal's Widespread Fire: Short- and Long-Term Implications for Biodiversity and Conservation. *Biodivers Conserv.* **2021**, *30*, 3299–3303. [[CrossRef](#)] [[PubMed](#)]
24. Menezes, L.S.; de Oliveira, A.M.; Santos, F.L.M.; Russo, A.; de Souza, R.A.F.; Roque, F.O.; Libonati, R. Lightning Patterns in the Pantanal: Untangling Natural and Anthropogenic-Induced Wildfires. *Sci. Total Environ.* **2022**, *820*, 153021. [[CrossRef](#)]
25. Leal Filho, W.; Azeiteiro, U.M.; Salvia, A.L.; Fritzen, B.; Libonati, R. Fire in Paradise: Why the Pantanal Is Burning. *Environ. Sci. Policy* **2021**, *123*, 31–34. [[CrossRef](#)]
26. Silgueiro, V.d.F.; Souza, C.O.C.F.d.; Muller, E.O.; Silva, C.J.d. Dimensions of the 2020 Wildfire Catastrophe in the Pantanal Wetland: The Case of the Municipality of Poconé, Mato Grosso, Brazil. *Res. Soc. Dev.* **2021**, *10*, e08101522619. [[CrossRef](#)]
27. Berlinck; Lima, L.H.A.; Pereira, A.M.M.; Carvalho, E.A.R.; Paula, R.C.; Thomas, W.M.; Morato, R.G. The Pantanal Is on Fire and Only a Sustainable Agenda Can Save the Largest Wetland in the World. *Braz. J. Biol.* **2021**, *82*. [[CrossRef](#)]
28. Garcia, L.C.; Szabo, J.K.; de Oliveira Roque, F.; de Matos Martins Pereira, A.; Nunes da Cunha, C.; Damasceno-Júnior, G.A.; Morato, R.G.; Tomas, W.M.; Libonati, R.; Ribeiro, D.B. Record-Breaking Wildfires in the World's Largest Continuous Tropical Wetland: Integrative Fire Management Is Urgently Needed for Both Biodiversity and Humans. *J. Environ. Manag.* **2021**, *293*, 112870. [[CrossRef](#)]
29. Correa, D.B.; Alcântara, E.; Libonati, R.; Massi, K.G.; Park, E. Increased Burned Area in the Pantanal over the Past Two Decades. *Sci. Total Environ.* **2022**, *835*, 155386. [[CrossRef](#)]
30. Daldegan, G.A.; Roberts, D.A.; Ribeiro, F.d.F. Spectral Mixture Analysis in Google Earth Engine to Model and Delineate Fire Scars over a Large Extent and a Long Time-Series in a Rainforest-Savanna Transition Zone. *Remote Sens. Environ.* **2019**, *232*, 111340. [[CrossRef](#)]
31. Marques, J.F.; Alves, M.B.; Silveira, C.F.; Amaral e Silva, A.; Silva, T.A.; dos Santos, V.J.; Calijuri, M.L. Fires Dynamics in the Pantanal: Impacts of Anthropogenic Activities and Climate Change. *J. Environ. Manag.* **2021**, *299*, 113586. [[CrossRef](#)]
32. Hoffmann, W.A.; Adasme, R.; Haridasan, M.; De Carvalho, M.T.; Geiger, E.L.; Pereira, M.A.B.; Gotsch, S.G.; Franco, A.C. Tree Topkill, Not Mortality, Governs the Dynamics of Savanna–Forest Boundaries under Frequent Fire in Central Brazil. *Ecology* **2009**, *90*, 1326–1337. [[CrossRef](#)]
33. Myers, R. *Convivendo Com o Fogo—Manutenção Dos Ecossistemas & Subsistência Com o Manejo Integrado Do Fogo*; The Nature Conservancy: Tallahassee, FL, USA, 2006.
34. Schmidt, I.B.; Eloy, L. Fire Regime in the Brazilian Savanna: Recent Changes, Policy and Management. *Flora* **2020**, *268*, 151613. [[CrossRef](#)]
35. Berlinck, C.N.; Helena, L.; Lima, A. Implementation of Integrated Fire Management in Brazilian Federal Protected Areas. *Biodivers. Bras. BioBrasil* **2021**, *11*, 128–138. [[CrossRef](#)]
36. Santos, A.C.d.; Montenegro, S.d.R.; Ferreira, M.C.; Barradas, A.C.S.; Schmidt, I.B. Managing Fires in a Changing World: Fuel and Weather Determine Fire Behavior and Safety in the Neotropical Savannas. *J. Environ. Manag.* **2021**, *289*, 112508. [[CrossRef](#)] [[PubMed](#)]
37. Santos, F.L.M.; Nogueira, J.; De Souza, R.A.F.; Falleiro, R.M.; Schmidt, I.B.; Libonati, R. Prescribed Burning Reduces Large, High-Intensity Wildfires and Emissions in the Brazilian Savanna. *Fire* **2021**, *4*, 56. [[CrossRef](#)]

38. Pivello, V.R. The Use of Fire in the Cerrado and Amazonian Rainforests of Brazil: Past and Present. *Fire Ecology* **2011**, *7*, 24–39. [[CrossRef](#)]
39. Cowman, D.; Russell, W. Fuel Load, Stand Structure, and Understory Species Composition Following Prescribed Fire in an Old-Growth Coast Redwood (*Sequoia Sempervirens*) Forest. *Fire Ecol.* **2021**, *17*, 1–13. [[CrossRef](#)]
40. Sonnier, G.; Boughton, E.H.; Whittington, R. Long-term Response of Wetland Plant Communities to Management Intensity, Grazing Abandonment, and Prescribed Fire. *Ecol. Appl.* **2023**, *33*. [[CrossRef](#)]
41. Beyene, M.T.; Leibowitz, S.G.; Dunn, C.J.; Bladon, K.D. To Burn or Not to Burn: An Empirical Assessment of the Impacts of Wildfires and Prescribed Fires on Trace Element Concentrations in Western US Streams. *Sci. Total Environ.* **2023**, *863*, 160731. [[CrossRef](#)] [[PubMed](#)]
42. Pérez-Rodríguez, L.A.; Quintano, C.; Marcos, E.; Suarez-Seoane, S.; Calvo, L.; Fernández-Manso, A. Evaluation of Prescribed Fires from Unmanned Aerial Vehicles (UAVs) Imagery and Machine Learning Algorithms. *Remote Sens* **2020**, *12*, 1295. [[CrossRef](#)]
43. Fernández-Guisuraga, J.M.; Sanz-Ablanedo, E.; Suárez-Seoane, S.; Calvo, L. Using Unmanned Aerial Vehicles in Postfire Vegetation Survey Campaigns through Large and Heterogeneous Areas: Opportunities and Challenges. *Sensors* **2018**, *18*, 586. [[CrossRef](#)] [[PubMed](#)]
44. Zhang, Y.; Onda, Y.; Kato, H.; Feng, B.; Gomi, T. Understory Biomass Measurement in a Dense Plantation Forest Based on Drone-SfM Data by a Manual Low-Flying Drone under the Canopy. *J. Environ. Manag.* **2022**, *312*, 114862. [[CrossRef](#)] [[PubMed](#)]
45. Fraser, R.H.; van der Sluijs, J.; Hall, R.J. Calibrating Satellite-Based Indices of Burn Severity from UAV-Derived Metrics of a Burned Boreal Forest in NWT, Canada. *Remote Sens.* **2017**, *9*, 279. [[CrossRef](#)]
46. Fillmore, S.D.; McCaffrey, S.M.; Smith, A.M.S. A Mixed Methods Literature Review and Framework for Decision Factors That May Influence the Utilization of Managed Wildfire on Federal Lands, USA. *Fire* **2021**, *4*, 62. [[CrossRef](#)]
47. Tomas, W.M.; Berlinck, C.N.; Chiaravalloti, R.M.; Faggioni, G.P.; Strüssmann, C.; Libonati, R.; Abrahão, C.R.; do Valle Alvarenga, G.; de Faria Bacellar, A.E.; de Queiroz Batista, F.R.; et al. Distance Sampling Surveys Reveal 17 Million Vertebrates Directly Killed by the 2020's Wildfires in the Pantanal, Brazil. *Sci. Rep.* **2021**, *11*, 1–8. [[CrossRef](#)]
48. Arruda, V.L.S.; Piontekowski, V.J.; Alencar, A.; Pereira, R.S.; Matricardi, E.A.T. An Alternative Approach for Mapping Burn Scars Using Landsat Imagery, Google Earth Engine, and Deep Learning in the Brazilian Savanna. *Remote Sens Appl.* **2021**, *22*, 100472. [[CrossRef](#)]
49. Pereira, G.; Longo, K.M.; Freitas, S.R.; Mataveli, G.; Oliveira, V.J.; Santos, P.R.; Rodrigues, L.F.; Cardozo, F.S. Improving the South America Wildfires Smoke Estimates: Integration of Polar-Orbiting and Geostationary Satellite Fire Products in the Brazilian Biomass Burning Emission Model (3BEM). *Atmos Environ.* **2022**, *273*, 118954. [[CrossRef](#)]
50. Chen, X.; Vogelmann, J.E.; Rollins, M.; Ohlen, D.; Key, C.H.; Yang, L.; Huang, C.; Shi, H. Detecting Post-Fire Burn Severity and Vegetation Recovery Using Multitemporal Remote Sensing Spectral Indices and Field-Collected Composite Burn Index Data in a Ponderosa Pine Forest. *Int. J. Remote Sens.* **2011**, *32*, 7905–7927. [[CrossRef](#)]
51. Samiappan, S.; Hathcock, L.; Turnage, G.; McCraine, C.; Pitchford, J.; Moorhead, R. Remote Sensing of Wildfire Using a Small Unmanned Aerial System: Post-Fire Mapping, Vegetation Recovery and Damage Analysis in Grand Bay, Mississippi/Alabama, USA. *Drones* **2019**, *3*, 43. [[CrossRef](#)]
52. Sherstjuk, V.; Zharikova, M.; Sokol, I. Forest Fire Monitoring System Based on UAV Team, Remote Sensing, and Image Processing. In Proceedings of the 2018 IEEE 2nd International Conference on Data Stream Mining and Processing, DSMP, Lviv, Ukraine, 21–25 August 2018; pp. 590–594. [[CrossRef](#)]
53. Nascente, J.C.; Ferreira, M.E.; Nunes, G.M. Integrated Fire Management as a Renewing Agent of Native Vegetation and Inhibitor of Invasive Plants in Vereda Habitats: Diagnosis by Remotely Piloted Aircraft Systems. *Remote Sens.* **2022**, *14*, 1040. [[CrossRef](#)]
54. Díaz-Delgado, R.; Cazacu, C.; Adamescu, M. Rapid Assessment of Ecological Integrity for LTER Wetland Sites by Using UAV Multispectral Mapping. *Drones* **2018**, *3*, 3. [[CrossRef](#)]
55. Nunes, G.M.; Thais, M.; Duarte De Siqueira, M. Análise Temporal de Macro-Habitat No Pantanal via Processamento de Fotografias Aéreas e Dados Obtidos Por Sistemas de Aeronaves Remotamente Pilotadas. *Biodivers. Bras. BioBrasil* **2019**, *9*, 71–85. [[CrossRef](#)]
56. Dabrowska-Zielinska, K.; Gruszczynska, M.; Lewinski, S.; Hoscilo, A.; Bojanowski, J. Application of Remote and in Situ Information to the Management of Wetlands in Poland. *J. Environ. Manag.* **2009**, *90*, 2261–2269. [[CrossRef](#)]
57. Carvajal-Ramírez, F.; Marques da Silva, J.R.; Agüera-Vega, F.; Martínez-Carricondo, P.; Serrano, J.; Moral, F.J. Evaluation of Fire Severity Indices Based on Pre- and Post-Fire Multispectral Imagery Sensed from UAV. *Remote Sens.* **2019**, *11*, 993. [[CrossRef](#)]
58. Allison, R.S.; Johnston, J.M.; Craig, G.; Jennings, S. Airborne Optical and Thermal Remote Sensing for Wildfire Detection and Monitoring. *Sensors* **2016**, *16*, 1310. [[CrossRef](#)]
59. Nasery, S.; Kalkan, K. Burn Area Detection and Burn Severity Assessment Using Sentinel 2 MSI Data: The Case of Karabağlar District, İzmir/Turkey. *Turk. J. Geosci.* **2020**, *1*, 72–77.
60. Stow, D.A.; Lippitt, C.D.; Coulter, L.L.; Loerch, A.C. Towards an End-to-End Airborne Remote-Sensing System for Post-Hazard Assessment of Damage to Hyper-Critical Infrastructure: Research Progress and Needs. *Int. J. Remote Sens.* **2018**, *39*, 1441–1458. [[CrossRef](#)]
61. Barbosa da Silva, F.H.; Arieira, J.; Parolin, P.; Nunes da Cunha, C.; Junk, W.J. Shrub Encroachment Influences Herbaceous Communities in Flooded Grasslands of a Neotropical Savanna Wetland. *Appl. Veg. Sci.* **2016**, *19*, 391–400. [[CrossRef](#)]

62. Nunes da Cunha, C.; Barbosa da Silva, F.H.; da Costa, C.P.; Junk, W.J. Woody Encroachment and Its Control in Periodically Flooded Grasslands of the Pantanal, a Large Brazilian Wetland. In *Flora and Vegetation of the Pantanal Wetland*; Springer: Berlin/Heidelberg, Germany, 2021; pp. 491–512. [CrossRef]
63. Garcia, L.; Zuquim, B.P.d.T.; Luiz, B.F.d.O.; Tereza, M.; Pádua, J.; da Costa Pereira, N.; Wolfgang Valutky, W. *Plano de Manejo Da Reserva Particular de Patrimônio Natural Do SESC Pantanal*, 2nd ed.; Garcia, L., Zuquim, P.d.T., Eds.; Pontificia Universidad Catolica del Peru: Rio de Janeiro, Brazil, 2011; ISBN 978-85-89336-30-7.
64. Cuiabá, R. *Vulnerabilidade Da Paisagem Pantaneira: Estudo de Caso Da Reserva Particular Do Patrimônio Natural Sesc Pantanal e Entorno*; Universidade de São Paulo: São Paulo, Brazil, 2016.
65. Alvares, C.A.; Stape, J.L.; Sentelhas, P.C.; de Moraes Gonçalves, J.L.; Sparovek, G. Köppen's Climate Classification Map for Brazil. *Meteorol. Z.* **2014**, *22*, 711–728. [CrossRef]
66. Moreira, R.; Vidal Torrado, P.; Luiz Stape, J.; Guimarães Couto, E.; Ramatis Plugiese Andrade, G. *Solos Da Reserva Particular Do Patrimônio Natural SESC Pantanal*; SESC, Departamento Nacional: Rio de Janeiro, Brazil, 2011; ISBN 85-89336-55-0.
67. Junk, W.J.; Piedade, M.T.F.; Lourival, R.; Wittmann, F.; Kandus, P.; Lacerda, L.D.; Bozelli, R.L.; Esteves, F.A.; Nunes da Cunha, C.; Maltchik, L.; et al. Brazilian Wetlands: Their Definition, Delineation, and Classification for Research, Sustainable Management, and Protection. *Aquat Conserv.* **2014**, *24*, 5–22. [CrossRef]
68. Nunes, C.; Fernandez, M.; Junk, W. *Classificação e Delimitação Das Áreas Úmidas Brasileiras e de Seus Macrohabitats*; Nunes da Cunha, C., Piedade, M.T.F., Junk, W.J., Eds.; EdUFMT: Cuiabá, Brazil, 2015; Volume 1.
69. Eloy, L.; Schmidt, I.B.; Borges, S.L.; Ferreira, M.C.; dos Santos, T.A. Seasonal Fire Management by Traditional Cattle Ranchers Prevents the Spread of Wildfire in the Brazilian Cerrado. *Ambio* **2018**, *48*, 890–899. [CrossRef] [PubMed]
70. Miranda, H.S. *Efeitos Do Regime Do Fogo Sobre a Estrutura de Comunidades de Cerrado: Resultados Do Projeto Fogo*; IBAMA: Brasília, Brazil, 2010; ISBN 978-85-7300-305-5.
71. MicaSense. *Altum Integration Guide—MicaSense Knowledge Base*, 10th ed.; Seattle, WA, USA, 2022; Available online: <https://support.micasense.com/hc/en-us> (accessed on 11 May 2023).
72. Biney, J.K.M.; Saberioon, M.; Borůvka, L.; Houška, J.; Vašát, R.; Agyeman, P.C.; Coblinski, J.A.; Klement, A. Exploring the Suitability of UAS-Based Multispectral Images for Estimating Soil Organic Carbon: Comparison with Proximal Soil Sensing and Spaceborne Imagery. *Remote Sens.* **2021**, *13*, 308. [CrossRef]
73. Bruce, R.W.; Rajcan, I.; Sulik, J. Classification of Soybean Pubescence from Multispectral Aerial Imagery. *Plant Phenomics* **2021**, *2021*, 1–11. [CrossRef] [PubMed]
74. Volke, M.I.; Abarca-Del-Rio, R. Comparison of Machine Learning Classification Algorithms for Land Cover Change in a Coastal Area Affected by the 2010 Earthquake and Tsunami in Chile. *Nat. Hazards Earth Syst. Sci.* **2020**, *41*, 1–14. [CrossRef]
75. Simpson, J.E.; Holman, F.; Nieto, H.; Voelksch, I.; Mauder, M.; Klatt, J.; Fiener, P.; Kaplan, J.O.; Wang, K.; Wang, Z. Remote Sensing High Spatial and Temporal Resolution Energy Flux Mapping of Different Land Covers Using an Off-the-Shelf Unmanned Aerial System. *Remote Sens.* **2021**, *13*, 1286. [CrossRef]
76. Rahaman, M.; Esraz-Ul-Zannat, M. Evaluating the Impacts of Major Cyclonic Catastrophes in Coastal Bangladesh Using Geospatial Techniques. *SN Appl. Sci.* **2021**, *3*, 727. [CrossRef]
77. Chuvieco, E.; Martín, M.P.; Palacios, A. Assessment of Different Spectral Indices in the Red-near-Infrared Spectral Domain for Burned Land Discrimination. *Int. J. Remote Sens.* **2002**, *23*, 5103–5110. [CrossRef]
78. Chen, Y.; Lara, M.J.; Hu, F.S. A Robust Visible Near-Infrared Index for Fire Severity Mapping in Arctic Tundra Ecosystems. *ISPRS J. Photogramm. Remote Sens.* **2020**, *159*, 101–113. [CrossRef]
79. Meng, R.; Wu, J.; Schwager, K.L.; Zhao, F.; Dennison, P.E.; Cook, B.D.; Brewster, K.; Green, T.M.; Serbin, S.P. Using High Spatial Resolution Satellite Imagery to Map Forest Burn Severity across Spatial Scales in a Pine Barrens Ecosystem. *Remote Sens. Environ.* **2017**, *191*, 95–109. [CrossRef]
80. Borges, K.M.R.; Orozco Filho, J.C.; Coan, G.P.d.O.; Vasconcelos, T.M.M. Sensoriamento Remoto e Geoprocessamento Como Subsídio Ao Manejo Do Fogo e Ao Combate Aos Incêndios Florestais Em Unidades de Conservação Federais. *Biodivers. Bras. BioBrasil* **2021**, *2*, 168–178. [CrossRef]
81. Klauberg, C.; Hudak, A.T.; Silva, C.A.; Lewis, S.A.; Robichaud, P.R.; Jain, T.B. Characterizing Fire Effects on Conifers at Tree Level from Airborne Laser Scanning and High-Resolution, Multispectral Satellite Data. *Ecol. Model.* **2019**, *412*, 108820. [CrossRef]
82. Woo, H.; Acuna, M.; Madurapperuma, B.; Jung, G.; Woo, C.; Park, J. Application of Maximum Likelihood and Spectral Angle Mapping Classification Techniques to Evaluate Forest Fire Severity from UAV Multi-Spectral Images in South Korea. *Sens. Mater.* **2021**, *33*, 3745–3760. [CrossRef]
83. Lenzi, I.L.C.; Nunes, G.M. Comparação Entre Os Classificadores Support Vector Machine e Spectral Angle Mapper Aplicado à Diferenciação Das Fitofisionomias Do Parque Estadual Do Araguaia (MT). *Rev. Georaguaiá* **2016**, *6*, 99.
84. Landis, J.R.; Koch, G.G. The Measurement of Observer Agreement for Categorical Data. *Biometrics* **1977**, *33*, 159. [CrossRef] [PubMed]
85. Hutton, J.J.; Lipa, G.; Baustian, D.; Sulik, J.; Bruce, R.W. High Accuracy Direct Georeferencing of the Altum Multi-Spectral Uav Camera and Its Application to High Throughput Plant Phenotyping. *Int. Arch. Photogramm. Remote Sens. Spat. Inf. Sci.* **2020**, *43*, 1–6. [CrossRef]
86. Chuvieco, E.; Mouillot, F.; van der Werf, G.R.; San Miguel, J.; Tanasse, M.; Koutsias, N.; García, M.; Yebra, M.; Padilla, M.; Gitas, I.; et al. Historical Background and Current Developments for Mapping Burned Area from Satellite Earth Observation. *Remote Sens. Environ.* **2019**, *225*, 45–64. [CrossRef]

87. Zanzarini, V.; Andersen, A.N.; Fidelis, A. Flammability in Tropical Savannas: Variation among Growth Forms and Seasons in Cerrado. *Biotropica* **2022**, *54*, 979–987. [[CrossRef](#)]
88. Fidelis, A. Is Fire Always the “Bad Guy”? *Flora* **2020**, *268*, 151611. [[CrossRef](#)]
89. Abreu, R.C.R.; Hoffmann, W.A.; Vasconcelos, H.L.; Pilon, N.A.; Rossatto, D.R.; Durigan, G. The Biodiversity Cost of Carbon Sequestration in Tropical Savanna. *Sci. Adv.* **2017**, *3*, e1701284. [[CrossRef](#)]
90. Newberry, B.M.; Power, C.R.; Abreu, R.C.R.; Durigan, G.; Rossatto, D.R.; Hoffmann, W.A. Flammability Thresholds or Flammability Gradients? Determinants of Fire across Savanna–Forest Transitions. *New Phytol.* **2020**, *228*, 910–921. [[CrossRef](#)] [[PubMed](#)]
91. Hoffmann, W.A.; Jaconis, S.Y.; McKinley, K.L.; Geiger, E.L.; Gotsch, S.G.; Franco, A.C. Fuels or Microclimate? Understanding the Drivers of Fire Feedbacks at Savanna–Forest Boundaries. *Austral Ecol.* **2012**, *37*, 634–643. [[CrossRef](#)]
92. Costa, Y.T.; Thomaz, E.L. Management, Sustainability and Research Perspective of Prescribed Fires in Tropical Parks. *Curr. Opin. Environ. Sci. Health* **2021**, *22*, 100257. [[CrossRef](#)]
93. Libonati, R.; Geirinhas, J.o.L.; Silva, P.S.; Russo, A.; Rodrigues, J.A.; Belém, L.B.C.; Nogueira, J.; Roque, F.O.; Dacamara, C.C.; Nunes, A.M.B.; et al. Assessing the Role of Compound Drought and Heatwave Events on Unprecedented 2020 Wildfires in the Pantanal. *Environ. Res. Lett.* **2022**, *17*, 015005. [[CrossRef](#)]
94. Arruda, W.D.S.; Oldeland, J.; Paranhos Filho, A.C.; Pott, A.; Cunha, N.L.; Ishii, I.H.; Damasceno, G.A. Inundation and Fire Shape the Structure of Riparian Forests in the Pantanal, Brazil. *PLoS ONE* **2016**, *11*, e0156825. [[CrossRef](#)]
95. Cruz, M.; Gould, J.; Hollis, J.; McCaw, W. A Hierarchical Classification of Wildland Fire Fuels for Australian Vegetation Types. *Fire* **2018**, *1*, 13. [[CrossRef](#)]
96. Gomes, L.; Miranda, H.S.; Silvério, D.V.; Bustamante, M.M.C. Effects and Behaviour of Experimental Fires in Grasslands, Savannas, and Forests of the Brazilian Cerrado. *For. Ecol. Manag.* **2020**, *458*, 117804. [[CrossRef](#)]
97. Marques, M.C.S.; Rodriguez, D.A. Impacts of the Landscape Changes in the Low Streamflows of Pantanal Headwaters–Brazil. *Hydrol Process* **2022**, *36*, e14617. [[CrossRef](#)]
98. Dorado-Rodrigues, T.F.; Layme, V.M.G.; Silva, F.H.B.; Nunes da Cunha, C.; Strüßmann, C. Effects of Shrub Encroachment on the Anuran Community in Periodically Flooded Grasslands of the Largest Neotropical Wetland. *Austral Ecol.* **2015**, *40*, 547–557. [[CrossRef](#)]
99. Eduardo Guimarães, C.; Léo Adriano, C.; Cátia, N.; Maria, L. *Estudo Sobre o Impacto Do Fogo Na Disponibilidade de Nutrientes, No Banco de Sementes e Na Biota de Solos Da RPPN SESC Pantanal*; Serviço, S., Ed.; SESC, Departamento Nacional: Rio de Janeiro, Brazil, 2006; Volume 1, ISBN 85-89336-17-4.
100. Pérez, C.C.; Olthoff, A.E.; Hernández-Trejo, H.; Rullán-Silva, C.D. Evaluating the Best Spectral Indices for Burned Areas in the Tropical Pantanos de Centla Biosphere Reserve, Southeastern Mexico. *Remote Sens. Appl.* **2022**, *25*, 100664. [[CrossRef](#)]
101. Carvajal-Ramírez, F.; Serrano, J.M.P.R.; Agüera-Vega, F.; Martínez-Carricondo, P. A Comparative Analysis of Phytovolume Estimation Methods Based on UAV-Photogrammetry and Multispectral Imagery in a Mediterranean Forest. *Remote Sens.* **2019**, *11*, 2579. [[CrossRef](#)]
102. Sanchez-Azofeifa, A.; Antonio Guzmán, J.; Campos, C.A.; Castro, S.; Garcia-Millan, V.; Nightingale, J.; Rankine, C. Twenty-First Century Remote Sensing Technologies Are Revolutionizing the Study of Tropical Forests. *Biotropica* **2017**, *49*, 604–619. [[CrossRef](#)]
103. Fernández-Guisuraga, J.M.; Calvo, L.; Fernandes, P.M.; Suárez-Seoane, S. Short-Term Recovery of the Aboveground Carbon Stock in Iberian Shrublands at the Extremes of an Environmental Gradient and as a Function of Burn Severity. *Forests* **2022**, *13*, 145. [[CrossRef](#)]
104. Libonati, R.; DaCamara, C.C.; Peres, L.F.; Sander de Carvalho, L.A.; Garcia, L.C. Rescue Brazil’s Burning Pantanal Wetlands. *Nature* **2020**, *588*, 217–219. [[CrossRef](#)] [[PubMed](#)]
105. Martins, P.I.; Belém, L.B.C.; Szabo, J.K.; Libonati, R.; Garcia, L.C. Prioritising Areas for Wildfire Prevention and Post-Fire Restoration in the Brazilian Pantanal. *Ecol. Eng.* **2022**, *176*, 106517. [[CrossRef](#)]
106. Franke, J.; Barradas, A.C.S.; Borges, M.A.; Menezes Costa, M.; Dias, P.A.; Hoffmann, A.A.; Orozco Filho, J.C.; Melchiori, A.E.; Siegert, F. Fuel Load Mapping in the Brazilian Cerrado in Support of Integrated Fire Management. *Remote Sens Environ.* **2018**, *217*, 221–232. [[CrossRef](#)]
107. Oliveira, A.S.; Soares-Filho, B.S.; Oliveira, U.; Van der Hoff, R.; Carvalho-Ribeiro, S.M.; Oliveira, A.R.; Scheepers, L.C.; Vargas, B.A.; Rajão, R.G. Costs and Effectiveness of Public and Private Fire Management Programs in the Brazilian Amazon and Cerrado. *For. Policy Econ.* **2021**, *127*, 102447. [[CrossRef](#)]
108. Barradas, A.C.S.; Torres Ribeiro, K. Manejo Integrado Do Fogo: Trajetória Da Estação Ecológica Serra Geral Do Tocantins (2001 a 2020). *Biodivers. Bras. BioBrasil* **2021**, *11*, 139–152. [[CrossRef](#)]
109. Ponzoni, F.; Zullo Junior, J.; Augusto Camargo Lamparelli, R. Calibração Absoluta Da Câmera CCD/CBERS-2. In Proceedings of the Anais XII Simpósio Brasileiro de Sensoriamento Remoto, Goiânia, Brasil, 16–21 April 2005; Instituto Nacional de Pesquisas Espaciais-INPE: Goiânia, Brazil, 2005; pp. 1067–1074. [[CrossRef](#)]

**Disclaimer/Publisher’s Note:** The statements, opinions and data contained in all publications are solely those of the individual author(s) and contributor(s) and not of MDPI and/or the editor(s). MDPI and/or the editor(s) disclaim responsibility for any injury to people or property resulting from any ideas, methods, instructions or products referred to in the content.